ELSEVIER

Sensors and Actuators B 21 (1994) 171–183

SENSORS AND ACTUATORS B CHEMICAL

Screen printing: a technology for the batch fabrication of integrated chemical-sensor arrays

Howard D. Goldberg[a,*], Richard B. Brown[a], Dong P. Liu[b], Mark E. Meyerhoff[b]

[a]*Department of Electrical Engineering and Computer Science, University of Michigan, Ann Arbor, MI 48109, USA*

[b]*Department of Chemistry, University of Michigan, Ann Arbor, MI 48109, USA*

Received 5 July 1993; in revised form 31 January 1994; accepted 8 February 1994

Abstract

The commercialization of integrated chemical sensors has been slowed by the difficulty of device encapsulation and membrane application. For reasons of both cost and reproducibility, the sensor-specific structures should be mass fabricated, as are the microelectronics. The challenge lies in merging the standard semiconductor process sequence with the non-standard steps used to form the transducers. We demonstrate that screen printing can be used to partition the fabrication into two distinct sequences, semiconductor processing and sensor-specific steps. This simplifies process development and evolution, and makes semiconductor foundry services available for manufacturing sensors. After conventional semiconductor processing, our wafers have silver epoxy contacts screen printed on the aluminum sensor pads; the silver forms a stable chemical interface to the membranes, and the epoxy makes a strong physical bond to them. Next, the polymeric membranes are applied and patterned with screen printing. Membranes of different compositions can be deposited on the various sites of a multisensor chip by simply repeating the screen print/cure cycle. We show that the electrochemical performance of mass-fabricated passive and active sensor arrays is comparable to that of conventional liquid-junction ion-selective electrodes.

Keywords: Batch fabrication; Chemical sensor arrays; Screen printing

1. Introduction

To succeed in the marketplace, integrated sensors must fill application needs reliably and cost effectively. The deposition of sensor-specific layers must be done cost effectively and reproducibly. To satisfy many present and future applications, chemical sensors should include integrated circuitry. This requires the deposition of the sensor-specific layers and the encapsulation of the devices to be compatible with mass fabrication and standard CMOS processing. A fabrication approach that decouples the semiconductor process sequence from the non-standard steps used to form the transducer(s) allows independent optimization of the processes [1]. The concept of process partitioning has been demonstrated in sensors where micromachined structures are merged with interface electronics [2].

The most common method for applying polymeric membranes to solid-state sensors has been solvent casting, which requires hand work under a microscope [3,4]. Given the small size of the sensors, this is a tedious task, and the source of greatest yield loss. Control of membrane thickness and shape is difficult, resulting in a lack of sensor reproducibility. Others have also addressed the problem of membrane application. A technique that involves conformally coating the chip with a blank membrane and selectively doping the membrane over the sensing sites has been reported [5]. This method requires large chip geometries to avoid electrode crosstalk in multisensing devices, and suffers from lateral diffusion of the ionophore over time. A photoresist lift-off method has resulted in precisely patterned membranes [6], but this technique exposes the membranes to organic lift-off solvents, which may alter their electrochemical characteristics, and the range of thicknesses is limited to those that can be realized in photoresist. Photolithographically patternable membranes have been reported [7], but they have poor adhesion to the metal electrodes and require comparatively large spaces between sensor sites. In a sensor array, this approach would expose membranes to cross-contamination as successive layers are applied. Computer-controlled syringe dispensing systems have been developed to deposit

*Author to whom correspondence should be addressed at the Microsystems Technology Laboratories, Massachusetts Institute of Technology, Bldg. 39-561, Cambridge, MA 02139, USA.

Elsevier Science S.A.
SSDI 0925-4005(94)01249-H

various sensor layers across a wafer [8,9]; the expected throughput rate is low, especially for wafers containing sensor arrays, and the resulting membranes are usually thin (i.e., 20 μm [8]), which shortens sensor lifetimes due to ionophore leaching.

To apply the sensor-specific layers reliably and cost effectively, we have employed screen printing. Initial results in patterning silver epoxy electrode contacts and polymeric membranes demonstrated the feasibility of this approach [10]. Our work benefitted from developments in the screen printing of polymers for passivation of electronic circuits [11]. Screen printing deposits the contacts or membranes on a full wafer at a time. It can form thick layers, has short cycle times, is reproducible, allows precise pattern control, and is additive (no waste of material). To make this method feasible, the membranes, which had already been optimized for electrochemical and adhesive properties [12–14], had to be optimized for screen printability. To be specific, we needed to modify the membrane paste in order to minimize lateral flow-out and yield thicker membranes. Based on this effort, an initial set of screen-printing parameters and limitations was presented for passive solid-state chemical sensor fabrication [15,16].

Others have reported the use of screen printing to deposit glass-based pastes for hybrid pH sensors [17–19] and to deposit conductive pastes to form the electrode layers for various hybrid chemical sensors [20–22]. These materials require firing temperatures above 800 °C to cure the deposited materials, so they cannot be integrated with CMOS circuitry – one of our goals for improving the manufacturability of chemical sensors.

This use of screen printing in the fabrication of chemical sensors has enabled the microsensor manufacturing sequence to be easily partitioned, as shown in Fig. 1. Conventional CMOS processing is used to form the on-chip electronics, after which overglass openings are made to the aluminum sensor pads at the same time as the bonding-pad regions are opened; screen printing is then used to deposit the sensor-specific layers. Screen printing adds rheological constraints to materials [23,24], but it eliminates the need for developing, etching, and lift-off, processing steps that are more complicated and might alter the electrochemical characteristics of the sensing layers. Furthermore, the materials involved can be applied and cured at relatively low temperatures, so that the sensor-specific steps can be done after CMOS processing. Recently, others have also used screen printing to form chemical transducers [25]; their relatively simple sensors were formed on large ceramic substrates.

To demonstrate the benefits of this new manufacturing technology, several types of sensor chips of varying complexity were designed and fabricated.

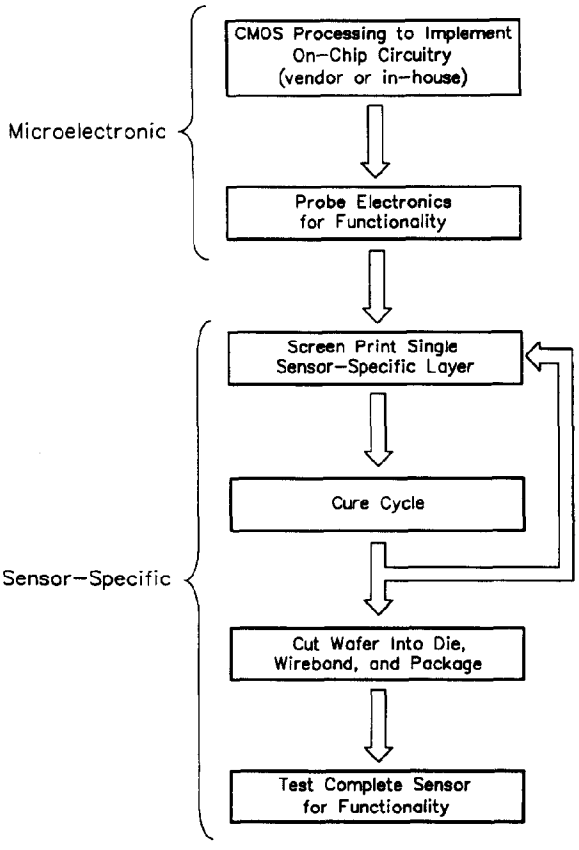

Fig. 1. Partitioned process flow for mass-fabricated sensor arrays.

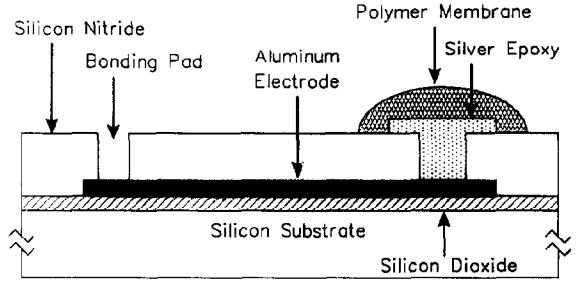

Fig. 2. Cross-sectional view of a solid-state microelectrode.

(1) The first of these were miniature, multi-site, ion-selective electrodes (ISEs) (the sensor cross section is shown in Fig. 2). Several clinical and environmental monitoring applications would benefit from the availability of low-cost/disposable passive chemical sensors like these that could be used with portable instrumentation.

(2) The second sensor type was a multisensor chip with four buffered ion-selective electrodes; a floorplan of this design is shown in Fig. 3. A control line switches the input between the transducer and system ground, allowing periodic calibration of the circuit offset potentials by the host controller. Such sensors are well

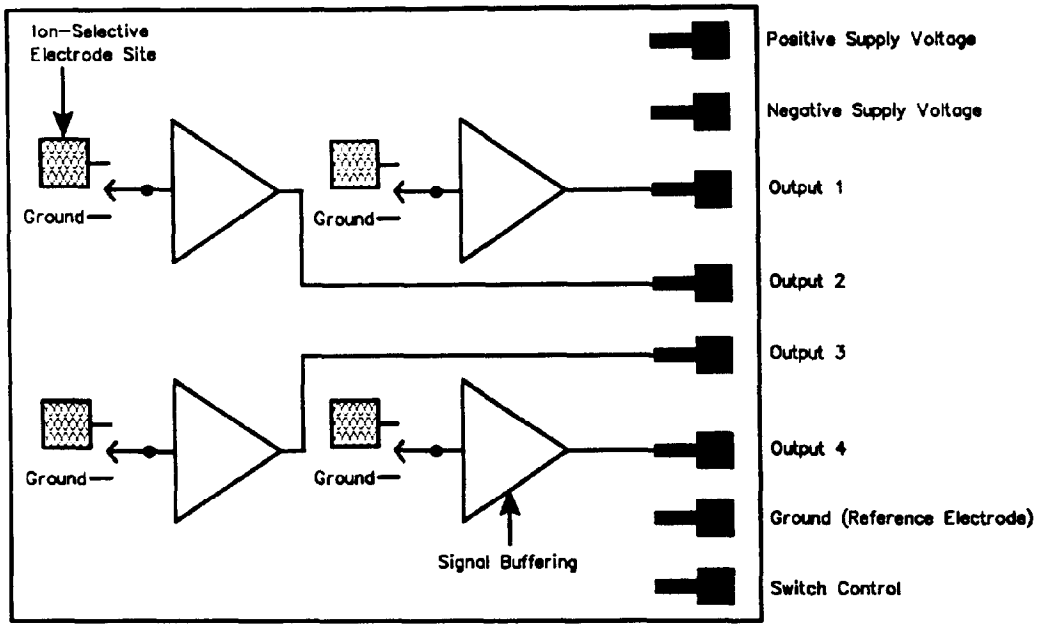

Fig. 3. Floorplan of the basic chemical multisensor chip.

suited to applications in industrial process control, the manufacture of foodstuffs, and the pharmaceutical industry, for example, which need remote sensors that can be readily configured by a control system (i.e., microcomputer or microcontroller) and can reliably communicate sensor data back to the host controller. The remote sensor effectively closes the system control loop, allowing the host controller to make real-time decisions that result in the initiation of actuator-driven control sequences.

(3) The third type of sensor is represented by Fig. 4. This programmable multisensor chip offers 14 user-programmable readout modes, a programmable gain stage, a 12-bit analog-to-digital converter, and an RS-422 serial communication interface. This stand-alone multisensor chip includes a temperature sensor and four buffered ion-selective electrode sites with switching circuitry at the inputs, which allow system ground or a reference voltage to be read. The sensor allows calibration for the temperature sensitivity of the electrochemical responses, and circuit offset and gain drift with time and temperature. This more complicated device can be configured for use in a wide range of applications.

Affordable sensor arrays such as these can provide multicomponent analysis, interference compensation, redundancy, and extended dynamic range.

There have been several reported attempts to fabricate the reference electrode on-chip with the sensing element; some of these efforts have included the deposition of silver/silver chloride films, the utilization of ISFETs/ISEs coated with hydrophobic ion-blocking polymer membranes [26], and the micromachining of liquid-junction reference electrodes [27,28]. Typically, microfabricated reference electrodes require specific operating conditions (i.e., constant chloride activity or pH range), exhibit significant drift of the reference potential, and/or have reproducibility problems. The nature of each individual sensing application determines the type of reference electrode that is required. Continuous on-line integrated sensors require the electrochemical stability of a conventional liquid-junction reference electrode. For most applications, the miniaturization of this reference electrode would be the most cost-effective approach for overall compatibility with planar mass-fabricated chemical sensors. This can be realized with either frit-tipped catheters with an internal wire and filling solution or injection-molded integrated sensor packages containing a liquid-filled chamber and plastic frit. Reference electrodes with short-term stability can be used with sensors in flow-injection systems, because such systems calibrate for the baseline drift of the electrochemical cell. Mass-fabricated chemical sensor arrays could also be considered as low-cost/replaceable parts to be plugged into portable instrumentation, which would already contain a high-quality reference electrode.

2. Polymeric membrane characterization

The two membrane pastes we characterized for screen printing are a polyurethane-based matrix PU/(PVC/Ac/Al), which had been previously optimized for adhesion and electrochemical performance, and a moisture-cu-

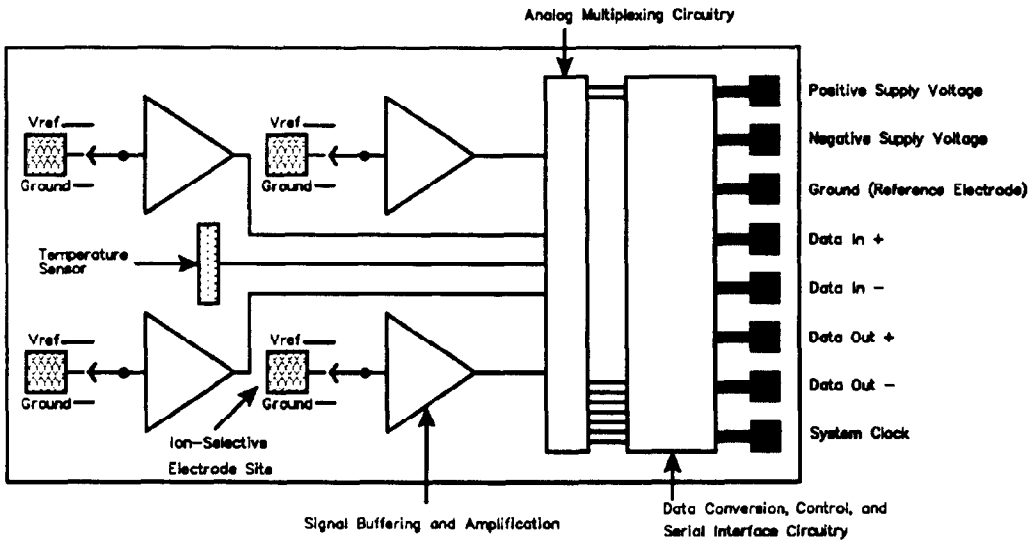

Fig. 4. Floorplan of the programmable chemical multisensor chip.

rable silicone rubber matrix, which also exhibits excellent adhesion and electrochemical characteristics. The preparation and electrochemical performance of the PU/(PVC/Ac/Al) membrane (matrix composition: PU 26.4 wt.%, 6.6 wt.% copolymer of vinyl chloride/vinyl acetate/vinyl alcohol (PVC/Ac/Al: 85/5/15 wt.%), 66 wt.% plasticizer, and 1 wt.% neutral carrier) have been previously reported by our research group [14]. The silicone rubber matrix is composed of 97.2 wt.% silicone rubber (RTV 3140; Dow Corning), 1 wt.% potassium tetrakis(p-chlorophenyl)borate, and 1.8 wt.% ionophore. This silicone rubber matrix offers lower membrane resistance than the Petrarch silicone rubber-based membrane matrix previously reported by our group [14]. Fig. 5 shows the structure of the polymer matrices used to prepare the ion-selective membrane pastes for the integrated chemical sensors.

The screen-printing process is illustrated in Fig. 6. Masks are composed of either a stainless-steel mesh coated with a photoreactive emulsion, or a metal-foil stencil. The screen printer applies the membrane paste evenly to the mask and rubs it with a squeegee, which pushes the paste through the openings in the mask onto the substrate. Solvents are used to achieve membrane paste with appropriate viscosity (for resistance to flow from squeegee motion) and thixotropy (for resistance to secondary flow after the mask is removed from the substrate) for good pattern definition. The membrane/solvent system plays a significant role in determining the screenability of the resulting paste. Anhydrous tetrahydrofuran (THF), which is commonly used to solvent-cast membranes, is unacceptable in a screen-printing membrane paste because its high solvent

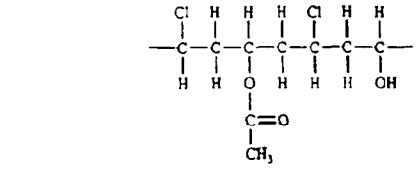

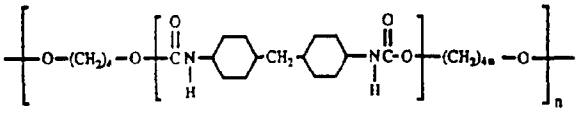

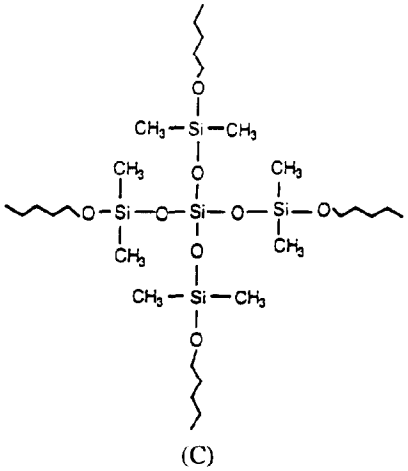

Fig. 5. Structure of the polymer matrices used for preparing ion-selective membrane pastes for the potentiometric chemical sensors: A, vinyl chloride/vinyl acetate/vinyl alcohol copolymer (PVC/Ac/Al); B, Tecoflex polyurethane; C, Dow Corning RTV 3140 silicone rubber.

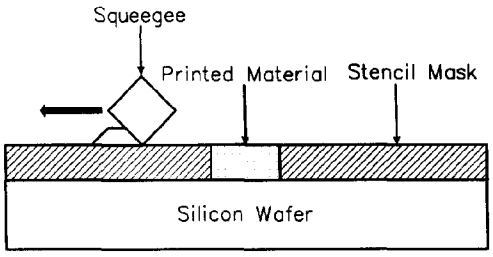

Fig. 6. The screen-printing process.

evaporation rate causes the viscosity of the paste to change rapidly, and it soon clogs the mask.

The use of higher boiling-point (i.e., lower evaporation rates) solvents such as N,N-dimethylacetamide (DMA) and cyclohexanone was investigated. Pastes composed of the PU/(PVC/Ac/Al) matrix dissolved in various combinations of DMA/THF and cyclohexanone/THF solvents were screen printed. The THF was used to dissolve the membrane components, after which it was evaporated from the final paste solution in a vacuum desiccator. Though viscosity was controlled with this mixture [10], the membrane pastes needed to be further optimized to reduce the flow-out of the printed membranes. As a result, 1-methyl-2-pyrrolidinone was investigated as a potential solvent system for the PU/(PVC/Ac/Al) membrane paste. As before, THF was added to the initial membrane solution and was later evaporated from the final membrane paste. Pastes with good viscosity and thixotropy were achieved with this solvent system. Though the higher boiling-point solvent resulted in a paste with good screenability, when silicon tetrachloride was added to the paste to increase membrane adhesion and improve the resulting electrode stability, the paste began to gel on the mask, probably because the $SiCl_4$ initiated cross-linking of the matrix.

Inert fillers such as silica powder are often employed to improve the rheology of screen-printing pastes [29,30]. Fumed silica powder (particle size 0.007 μm; Sigma Chemical Co.) was added to the polyurethane-based membrane to improve its pattern definition. Because a large percentage of silica powder had to be added to achieve the desired viscosity, the resulting membranes had numerous pinholes and irregularities.

In another effort, the total amount of solvent was reduced in order to increase the paste viscosity and thixotropy: this was expected to yield thicker membranes with reduced lateral flow-out. As the solvent amount was decreased, the paste became tacky and stringy and began to gel on the mask, making screen printing difficult. The screen-printing process increases the solvent evaporation rate as it spreads a thin layer of the paste onto the screen mask, increasing the amount of surface area of the membrane paste exposed to the air. This effect sets a bound on how much solvent had to be used in the paste; the resulting membranes were thinner and had poorer pattern definition than was acceptable.

Good screen-printing results were finally achieved by using PI-Thinner (Epoxy Technology), a proprietary mixture of various high boiling-point solvents, in the membrane paste. The PU/(PVC/Ac/Al) components (66 mg of polymeric material) are first completely dissolved in 1.2 ml of THF, after which 0.1 ml of PI-Thinner is added and mixed thoroughly. The low boiling-point THF is evaporated from the resulting membrane paste and 7 wt.% of $SiCl_4$ is added just prior to screen printing. The past exhibits good screenability, membrane thickness, and pattern definition. The cure cycle consists of a 1 h convection oven bake at 70 °C to accelerate the PI-Thinner evaporation process, followed by a room-temperature cure for 24 h.

In contrast to the polyurethane-based membranes, silicone rubber membrane pastes are easier to prepare for screen printing. The silicone rubber membrane components are first completely dissolved in 1.2 ml of THF. The THF is evaporated and the resulting paste is ready for screen printing. No $SiCl_4$ is added to this matrix, since the membrane adhesion is excellent and the adhesion promoter significantly reduces the electrochemical response of these membranes. This reduction in electrochemical response may be the result of increased membrane self-adhesion (hindering the ion-exchange process); the silicone rubber contains trimethylated silica and hydroxyl-terminated polydimethylsiloxane (refer to Fig. 5C), which may react with $SiCl_4$. The silicone rubber paste exhibits better viscosity and thixotropy than the PU/(PVC/Ac/Al) paste. The silicone rubber membranes are cured at room temperature for 24 h to allow the vulcanizing process to occur.

3. Screen-printing parameters

Stainless-steel stencil masks (Micro-Screen, Inc.) were chosen to print the silver epoxy electrode contact (H20E; Epoxy Technology) and the polymer membranes on the solid-state sensors. The stencil masks offer longer lifetimes and better solvent resistance than emulsion masks. The thickness of pre-cured patterned layers is ideally determined by the mask thickness, which can be specified over a 25–250 μm range. Screens and printing equipment now available allow alignment and reproducibility to ± 5 μm. The screen printer used in this work is semi-automated and optically aligned (LS-15TV; New Long Co.). The throughput rate (set-up, test print for alignment purposes, alignment, and print) is approximately 5 min per wafer; this is independent of the number of sensor die on the wafer.

The print quality of the deposited material is a function of mask clearance from the substrate, squeegee

Table 1
Screen-printing parameters

Parameter	Silver epoxy	PU/(PVC/Ac/Al)	Silicone rubber
Mask clearance (mm)	0	0	0
Squeegee shape	diamond	square edge	square edge
Squeegee speed (mm/s)	100	100	150
Squeegee pressure (kg/cm^2)	0.9	1.0	1.1
Squeegee angle	none	60°	60°
Push-in quantity (mm)	0.1	0.1	0

speed, squeegee shape, squeegee angle, squeegee pressure, and squeegee push-in quantity. We have found that the edge quality of the pattern is influenced most by the squeegee shape and mask clearance from the substrate. Pattern flow-out and thickness are determined primarily by squeegee speed, pressure, and push-in quantity. If the squeegee speed is too fast or there is not enough pressure or push-in quantity, the pattern may not be completely filled by the paste, and the deposited material may form peaks instead of having a smooth profile. If the speed is too slow and the pressure or push-in quantity is too great, the flow-out will increase and the pattern thickness may decrease due to the 'scavenging' effects of the squeegee.

Even though silver epoxy is commercially available as a screen-printable paste, the silver epoxy printing parameters had to be carefully optimized, along with those for the polymeric membranes. Table 1 lists the optimized screen-printing parameters used to print the various sensor layers. The silver epoxy was cured for 15 min in a 150 °C oven. These parameters have to be adjusted slightly from run to run to account for slight variations in the rheology of the membrane paste.

The pattern-definition quality of the respective sensor layers is summarized in Table 2; the lateral flow-out numbers (in each direction) are the average value ± standard deviation. Lateral flow-out was determined by an automatic surface profilometer (Sloan DekTak II) and film thickness was determined by a scanning electron microscope (SEM) image of the cleaved sample. Smaller printed features tend to flow-out less, and tend to be thinner than larger features; this is most likely due to the increased influence of edge effects of the mask aperture, in conjunction with the wet-paste mask adhesion. We have found that pattern definition and control are poor when feature dimensions are smaller than 200 μm squares.

Table 2
Screen-printed pattern definition

Parameter	Silver epoxy	PU/(PVC/Ac/Al)	Silicone rubber
Mask thickness* (μm)	76	127	127
Layer thickness (μm)	40	83	137
Lateral flow-out (μm)	25 ± 16	66 ± 12	48 ± 10

*Vendor specification is ±12.7 μm.

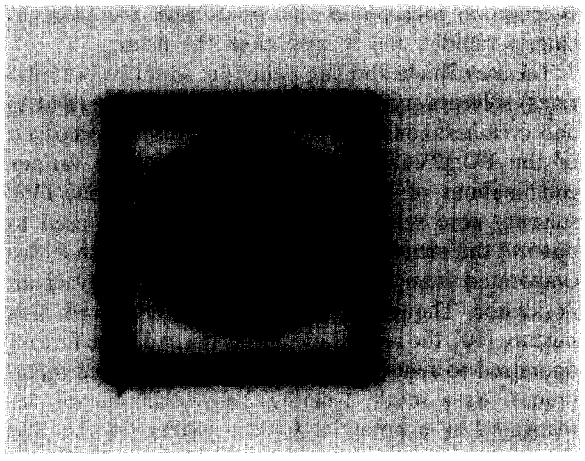

Fig. 7. A screen-printing epoxy wall used to minimize membrane flow-out. The walls are 20 μm thick with an average width of 129 ± 10 μm.

The feature definition of our membrane pastes is comparable to that of commercially available screen-printable pastes (e.g., Epoxy Technology 600SD polyimide printed 50 μm thick will yield 50 μm of flow-out [30]). The pattern definition achieved is within the tolerances needed for implementing most integrated chemical sensors. For applications requiring more closely spaced sensor sites, an epoxy wall can be printed, after the electrode contacts, to contain the membrane as shown in Fig. 7. An emulsion-coated screen mask (Micro-Screen) was used to form the wall layers. The epoxy (H54; Epoxy Technology) is extremely water resistant and offers high electrical resistivity, minimizing cross-talk on multi-site sensors. Preliminary work suggests that this epoxy wall concept could be especially helpful for precisely patterning bio-selective electrode sites with multiple membrane layers or a membrane layer coated with an enzyme-loaded gel.

4. Screen-printed sensor results

4.1. Passive chemical sensors

Miniature ion-selective electrodes having aluminum conductor lines and a low-temperature encapsulation

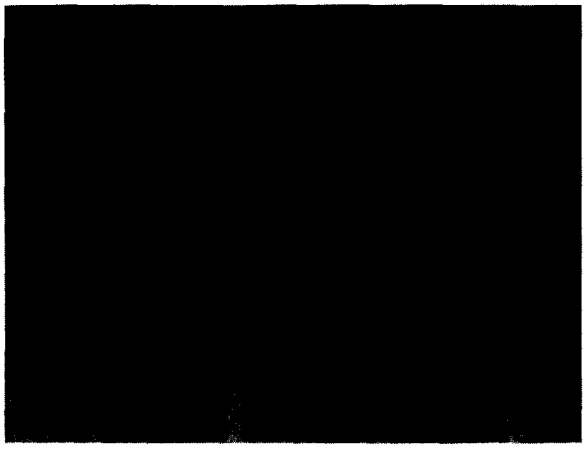

Fig. 8. Multi-site electrode with screen-printed silicone rubber membranes. For reference, the aluminum conductor lines are 110 μm wide.

scheme (spin-on-glass and plasma-deposited silicon nitride) were fabricated with a CMOS-compatible technology. Fig. 8 shows a multi-site electrode chip with screen-printed silicone rubber membranes; two membrane sizes were printed. To evaluate the electrochemical response, each multi-site electrode chip was wirebonded to a printed-circuit-board stalk, which facilitates the connection of external electrical leads. The wire bonds were the only part of the packaged sensor that required hand encapsulation, and this was achieved by the simple application of an epoxy composite (a combination of Devcon 2-Ton Epoxy and Hysol Epoxi-Patch 1C resulted in a good thermic seal).

To demonstrate the performance of a true multi-site sensor, four distinct ISE sites were implemented by screen printing potassium-selective (ionophore was valinomycin), calcium-selective (ionophore was ETH 129), ammonium-selective (ionophore was nonactin), and pH-responsive (ionophore was tridodecylamine) silicone rubber membranes. The calibration responses for two multisensor chips towards potassium, calcium, ammonium, and hydrogen ions are shown in Figs. 9–12, respectively. All of the sensors exhibited good electrochemical characteristics and the average sensor response slope was 59.3 mV/decade for potassium; calcium was 18 mV/decade; ammonium was 53.4 mV/decade; and pH was 79.4 mV/decade. The calcium ion response was sub-Nernstian, but still useful, and it was determined that the procedure used to accelerate the wirebond epoxy curing (90 °C convection oven cure for 30 min) had some effect on the electrochemical properties of the ETH 129 ionophore. Currently, packaged sensors undergo a lengthier room-temperature cure cycle. The silicone rubber matrix was known to exhibit some inherent pH sensitivity, which is due to the presence of hydroxyl-terminated components in the matrix (see

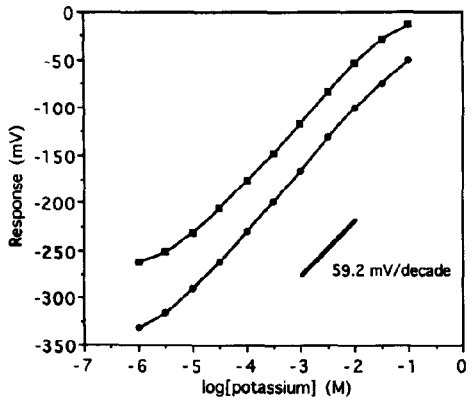

Fig. 9. Potassium-ion response for two multi-site electrodes. For comparison, the ideal Nernstian response of 59.2 mV/decade is shown.

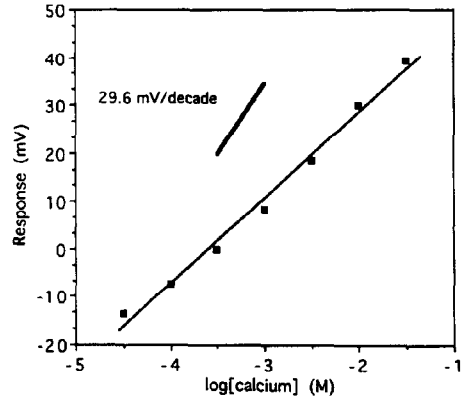

Fig. 10. Calcium-ion response for a multi-site electrode. For comparison, the ideal Nernstian response of 29.6 mV/decade is shown.

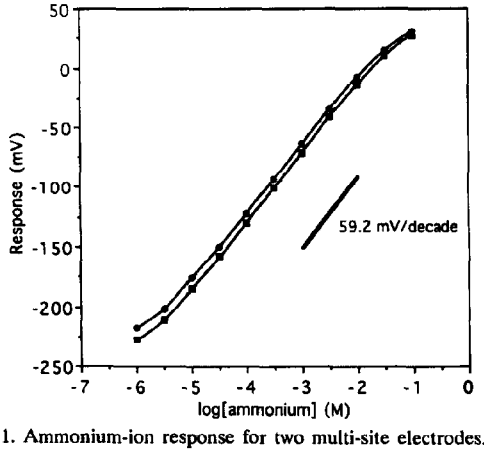

Fig. 11. Ammonium-ion response for two multi-site electrodes. For comparison, the ideal Nernstian response of 59.2 mV/decade is shown.

Fig. 5C); this was responsible for the super-Nernstian response characteristics of our hydrogen-selective sensors. The average selectivity coefficients for the two multi-site electrodes are listed in Table 3. These se-

Table 3
Selectivity coefficients for the screen-printed passive sensor arrays

$\log k_{ij}^{pot}$									
$i=K^+$			$i=NH_4^+$			$i=Ca^{2+}$		
$j-NH_4^+$	$j-Ca^{2+}$	$j-H^+$	$j-K^+$	$j-Ca^{2+}$	$j-H^+$	$j-NH_4^+$	$j-K^+$	$j-H^+$
−1.81	−3.48	−3.60	−0.73	−4.28	−3.68	−1.89	−2.78	−4.57

Note: selectivity data could note be obtained for the pH-responsive electrode sites because the evaluations of the potassium, ammonium, and calcium ion responses were done in Tris-HCl buffer solution (pH=7.2).

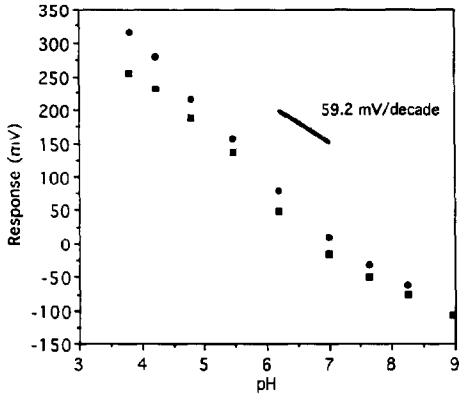

Fig. 12. Hydrogen-ion response for two multi-site electrodes. For comparison, the ideal Nernstian response of 59.2 mV/decade is shown.

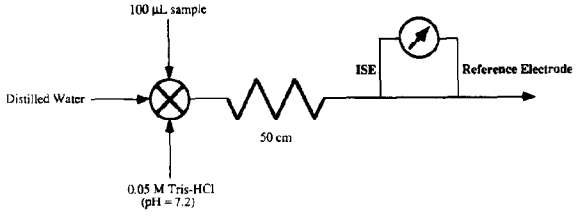

Fig. 13. Schematic of the flow-injection system.

lectivity coefficients, which are consistent with published selectivity data [31], show that the screen-printing process does not cross-contaminate the membranes and that sensors with good electrochemical responses can be obtained.

The external reference electrode was an Orion sleeve-type double-junction Ag/AgCl electrode (model 90-02). The sensor arrays were connected through a high-impedance amplifier to a Zenith Z-100 PC computer equipped with an analog-to-digital converter (DT 2801, Data Translations, Inc., Malborough, MA). Calibration data were obtained from additions of standard solutions to 250 ml of background electrolyte (0.05 M Tris-HCl, pH 7.2).

These multi-site electrodes were also used as an array detector in a wall-jet flow-injection system (schematic is shown in Fig. 13). The system injected 100 µl of various concentrations of NH_4Cl into a water carrier stream, which was merged with a stream of 0.05 M Tris-HCl buffer and then passed through a 50 cm mixing coil before reaching the flow cell. The flow-injection response of the sensor towards different concentrations of ammonium ions is shown in Fig. 14. The sensor performed continuously over 24 h with no change in its electrochemical response. Its response characteristics were equivalent to those obtained from the static mode experiments.

4.2. Active chemical sensors

Fig. 15 is a schematic cross section of a single electrode site on the active multisensor chips (floorplans are

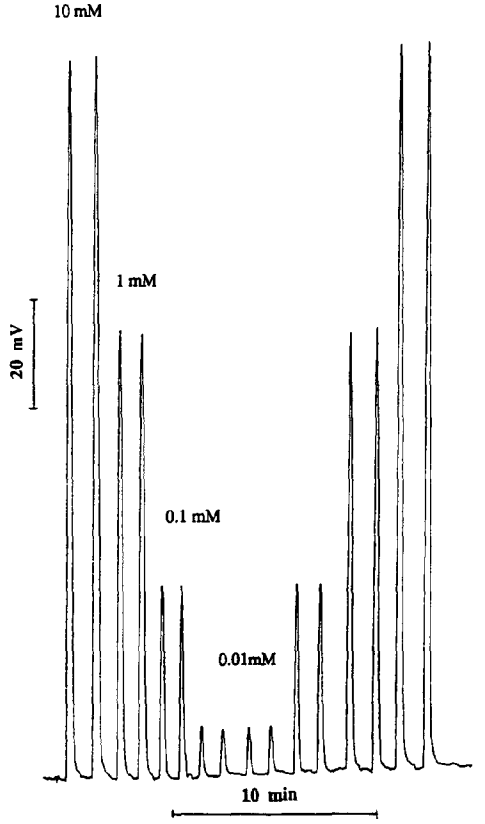

Fig. 14. Response obtained from flow-injection analysis for the multi-site electrode.

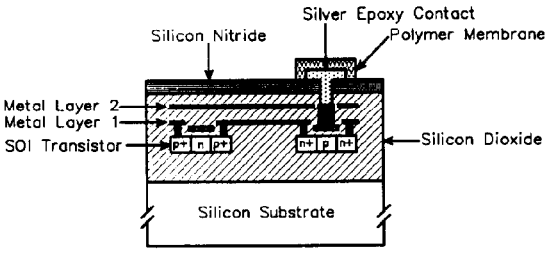

Fig. 15. Cross section of a single electrode site on the active multisensor chips.

shown in Figs. 3 and 4). Signals from the individual ion-selective electrode sites feed directly below to the input transistors of the amplification circuitry. These integrated ion-selective electrodes are well suited for most multisensing applications, since they have linear transfer characteristics and allow a common solution potential (i.e., common reference electrode). These features stand in contrast to those of ISFETs, which have nonlinear transfer characteristics; to prevent this nonlinearity from being superimposed on the chemical response, a feedback circuit typically drives the gate electrode [3]. Since each device would need to drive the solution with a different potential, simultaneous operation of sensor arrays is prohibited unless supported with complicated electronics. Furthermore, thermal sensitivity and photoinduced junction leakage currents cause calibration drifts in ISFETs.

Past efforts to encapsulate solid-state sensors have involved hand encapsulation with coatings [32], the use of expensive flow-cell packages [33], masked-epoxy techniques [34], hybrid-package bonding [35], electrochemical deposition [36], and junction-isolated semiconductor processes [3]; none of these schemes has achieved cost-effective mass production of the sensors and most do not achieve three-dimensional encapsulation. The circuitry on these multisensor chips was implemented on SOI substrates using a 2 μm, double-metal, double-polysilicon, p-well CMOS process developed in our Solid-State Electronics Laboratory. Each individual sensor chip is intrinsically encapsulated by dielectric layers as shown in Fig. 15 (the sensor surface was encapsulated with CMOS-compatible spin-on-glass and plasma-deposited silicon nitride layers).

As a result of the oxide isolation, SOI transistors also exhibit smaller junction leakage currents because of the reduced junction areas. For example, assuming 2 μm layout rules and 0.25 μm junction depths, a bulk CMOS transistor will have at least nine times more junction-leakage area than an equivalent SOI transistor. Because the ISEs on our multisensor chips are connected to the analog buffers via analog switches, reduced junction leakage is critical for good sensor performance.

The same silicone rubber-based membrane matrices that were screen printed on the passive sensor arrays were also printed on both active multisensor chips. The resulting basic multisensor chip with input switching circuitry and four operational amplifier buffers is shown in Fig. 16. The second metal layer was used to form a ground shield, preventing long-term dielectric breakdown of the silicon nitride encapsulation layer and reducing noise pick-up on the signal wires from the high-impedance ISEs. Fig. 17 is a photomicrograph of the programmable multisensor chip, with on-chip temperature sensor, programmable readout modes, serial communication interface, A/D converter, and programmable gain stage. For this chip, the second level of metallization was used as a routing layer for implementation of the relatively more complex circuitry, increasing the functional density of the die.

To evaluate the electrochemical response, each sensor chip was wirebonded to either a printed-circuit-board stalk or a ceramic dual-in-line package (Kyocera KD-S88422). Since the devices are self-encapsulating, only the wirebonds had to be hand encapsulated with epoxy. The potassium, calcium, and pH responses from the basic multisensor chip are shown in Fig. 18. The response characteristics are extremely linear; the correlation coef-

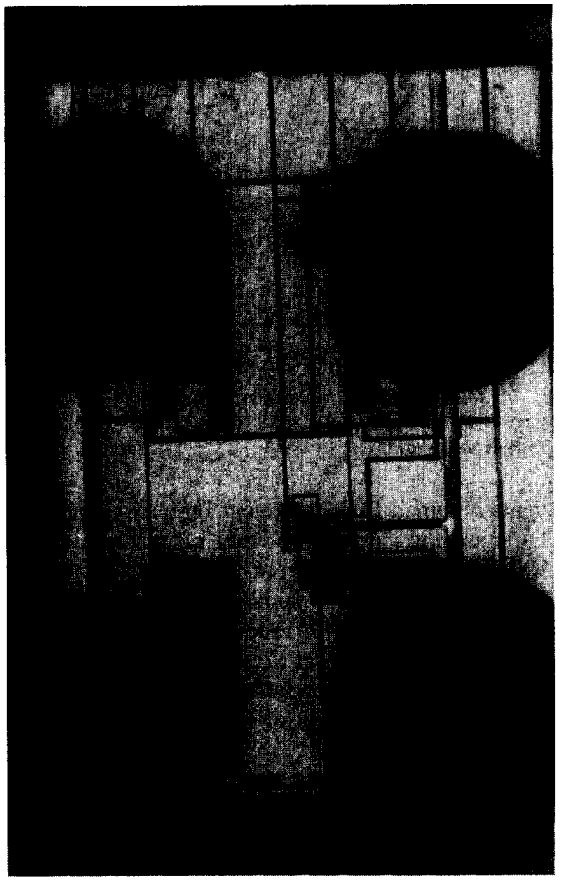

Fig. 16. Photomicrograph of the active chemical multisensor chip. The total die size is 1.7 mm×2.5 mm.

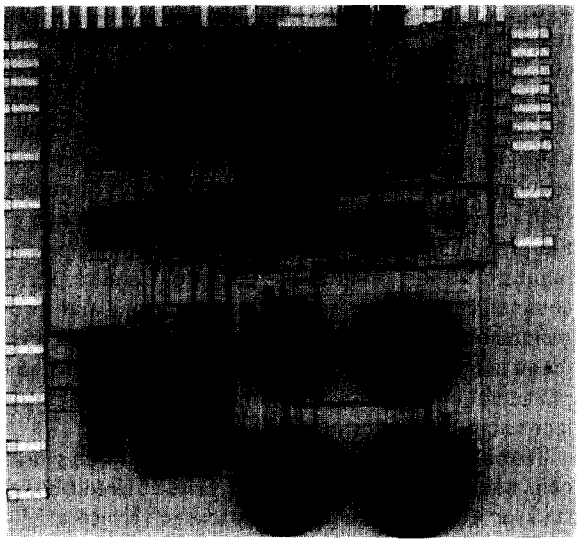

Fig. 17. Photomicrograph of the programmable chemical sensor chip. The die size is 5.8 mm × 6.0 mm; the circuit includes 4917 transistors.

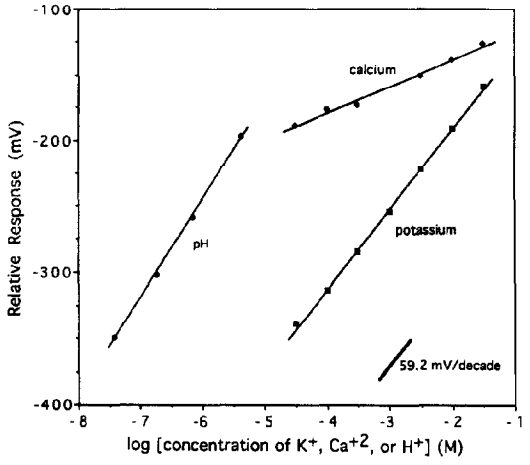

Fig. 18. Multisensor chip potassium, calcium, and hydrogen ion responses. For comparison, the ideal Nernstian response of 59.2 mV/decade is also shown.

ficients obtained from the linear regression analysis of the potassium, calcium, and pH responses are 1.000, 0.990, and 0.999, respectively. The potassium, calcium, and pH active sensor responses are 62.0 mV/decade, 20.3 mV/decade and 74 mV/decade, respectively. These electrochemical responses are comparable to those obtained from the passive chemical sensors, which illustrates the reproducibility of the screen-printing technique.

Fig. 19 shows both the measured sensor circuit response and the response calibrated for the analog offset drift of the system with temperature, using the operational amplifier buffer input switching circuit with a constant voltage forced on the ISE input. A 1 mV change in the ISE signal as the result of circuit offset

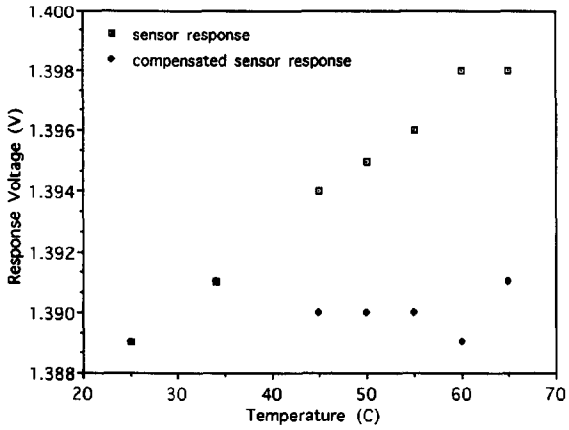

Fig. 19. Measured sensor circuit response vs. temperature and the circuit response with calibration for the analog offset drift.

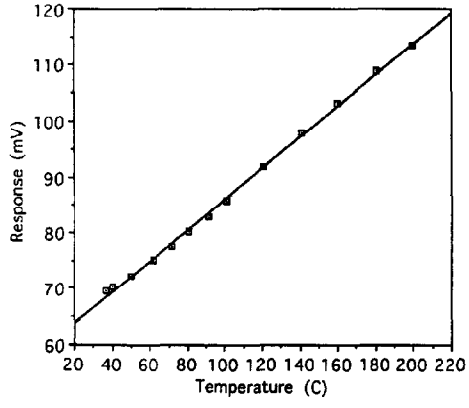

Fig. 20. Temperature sensor response.

corresponds to about a 4% change in concentration of the ion being monitored (assuming monovalent ion response). Similarly, the on-chip bandgap voltage reference of the programmable sensor chip allows calibration for analog gain drifts with time and temperature. The linear 0.27 mV/°C response of the on-chip temperature sensor is shown in Fig. 20; the gain of the on-chip instrumentation amplifier ($G = 18$) could be used to increase the overall response to 4.9 mV/°C. This capability of calibrating the electrochemical response for circuit- and temperature-induced effects results in sensors having greater accuracy and functionality which, in turn, allows them to address a larger range of potential applications.

5. Conclusions

The sensor-specific layers (silver epoxy solid-electrode contacts and polymeric membranes) were deposited after semiconductor processing with screen printing. This new sensor-fabrication methodology effectively partitions the process flow into two distinct and decoupled

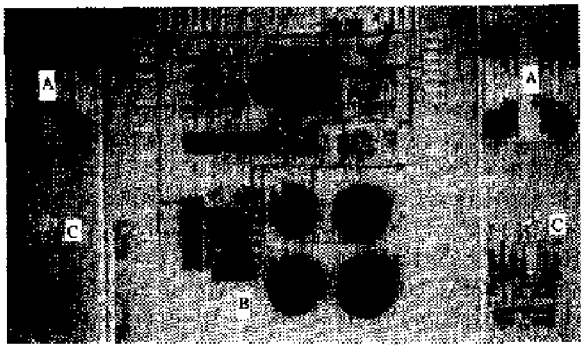

Fig. 21. Portion of an SOI CMOS wafer showing the implementation of two basic potentiometric chemical sensor arrays (A), a programmable potentiometric chemical sensor array (B), and two amperometric chemical sensors (C).

sequences, making the process more flexible and easing the technology transfer to industry. This approach allows various combinations of ion- and even bio-selective electrode sites to be implemented on a single multisensor chip. Screen printing even accommodates different types of chemical sensor arrays on a semiconductor wafer. For example, Fig. 21 is a photomicrograph of a portion of an SOI CMOS wafer containing two basic potentiometric chemical-sensor arrays, a programmable potentiometric chemical-sensor array, and two amperometric chemical sensors.

In conclusion, the most significant result of this work is the development of a technology that allows the mass production of cost-effective sensor arrays as well as sophisticated self-encapsulating integrated sensors. We believe that this will enable many industrial, environmental, and medical applications that need affordable, reliable, integrated chemical sensors.

Acknowledgements

We gratefully acknowledge the support of this work by Fleck Controls, Inc., Brookfield, WI, and by the National Science Foundation. Mr Robert W. Hower and Mr Michael E. Poplawski were involved with various aspects of the SOI CMOS process development. Dr Guen Sig Cha did the initial membrane development and was involved with the initial characterization of the screen-printing process. We also thank the KOPIN Corp. for generously providing the SOI wafers used to fabricate our integrated sensors, and Mr Derryl Allman at the NCR Microelectronics Division for his assistance with the development of our spin-on-glass technology.

References

[1] S.D. Senturia and R.L. Smith, Microsensor packaging and system partitioning, *Sensors and Actuators, 15* (1988) 221–234.

[2] K.D. Wise and N. Najafi, The coming opportunities in microsensor systems, *Tech. Digest, 6th Int. Conf. Solid-State Sensors and Actuators (Transducers '91), San Francisco, CA, USA, June 24–28, 1991*, pp. 2–7.

[3] R.B. Brown, An integrated multiple-sensor chemical transducer, *Ph.D. Thesis*, University of Utah, USA, June 1985.

[4] J. Kimura, T. Kuriyama and Y. Kawana, An integrated SOS/FET multi-biosensor and its application to medical use, *Tech. Digest, 3rd Int. Conf. Solid-State Sensors and Actuators, Transducers '85, Philadelphia, PA, USA, June 7–9, 1985*, pp. 152–155.

[5] K. Bezegh, A. Bezegh, J. Janata, A. Xu and W. Simon, Multisensing ion-selective field-effect transistors prepared by ionophore doping technique, *Anal. Chem., 59* (1987) 2846–2848.

[6] S. Nakamoto, N. Ito, T. Kuriyama and J. Kimura, A lift-off method for patterning enzyme-immobilized membranes in multibiosensors, *Sensors and Actuators, 13* (1988) 165–172.

[7] A. van den Berg, M. Koudelka-Hep, B. van der Schoot, E. Verney-Norberg, P. Krebs, A. Grisel and N. de Rooij, An on-wafer fabricated free-chlorine sensor, *Tech. Digest, 6th Int. Conf. Solid-State Sensors and Actuators (Transducers '91), San Francisco, CA, USA, June 24–28, 1991*, pp. 233–236.

[8] S. Anna, C. Li, Z. Zhilong, L. Luna and C. Keming, An IC-technology compatible automatic method (SCZ method) for immobilization membranes, *Sensors and Actuators, B1* (1990) 514–517.

[9] S.N. Cozette, G. Davis, J. Itak, I. Lauks, R. Mier, S. Piznik, N. Smit, S. Steiner, P. van der Werf and H. Wieck, Method of manufacturing a plurality of uniform microfabricated sensing devices having an immobilized ligand receptor, *US Patent No. 50 063 081* (Nov. 5, 1991).

[10] H.D. Goldberg, G.S. Cha, R.W. Hower and R.B. Brown, Batch fabrication of solid-state ion-selective sensors, *Tech. Digest, 3rd Int. Meeting Chemical Sensors, Cleveland, OH, USA, Sept. 1990*, pp. P31–P32.

[11] F.W. Kulesza, R.H. Estes and K. Spanjer, A screen-printable polyimide coating for silicon wafers, *Solid State Technol., 31* (1988) 135–139.

[12] H.D. Goldberg, G.S. Cha and R.B. Brown, Ion-selective sensors incorporating strongly adhesive polymeric membranes, *Tech. Digest, IEEE Sensor and Actuator Workshop, Hilton Head Island, SC, USA, June 1990*, pp. 169–172.

[13] H.D. Goldberg, G.S. Cha, D.P. Liu, M.E. Meyerhoff and R.B. Brown, Improved stability at the polymeric membrane/solid-contact interface of solid state potentiometric ion-sensors, *Tech. Digest, 6th Int. Conf. Solid-State Sensors and Actuators (Transducers '91), San Francisco, CA, USA, June 24–28, 1991*, pp. 781–784.

[14] G.S. Cha, D. Liu, M.E. Meyerhoff, H.C. Cantor, A.R. Midgley, H.D. Goldberg and R.B. Brown, Electrochemical performance, biocompatibility, and adhesion of new polymer matrices for solid-state ion sensors, *Anal. Chem., 63* (1991) 1666–1672.

[15] H.D. Goldberg, D.P. Liu, R.W. Hower, M.E. Poplawski and R.B. Brown, Screen printing: a technology for partitioning integrated microsensor processing, *Tech. Digest, IEEE Sensor and Actuator Workshop, Hilton Head Island, SC, USA, June 1992*, pp. 140–143.

[16] R.B. Brown, G.S. Cha and H.D. Goldberg, Batch deposition of polymeric ion sensor membranes, *US and Int. Patents Pending* (Aug. 20, 1991).

[17] R.E. Belford, A.E. Owen and R.G. Kelly, Thick-film hybrid pH sensors, *Sensors and Actuators, 11* (1987) 387–398.

[18] S.S. Yee and M.A. Afromowitz, in P.W. Cheung, D.G. Fleming, M.R. Neuman and W.H. Ko (eds.), *Theory, Design and Biomedical Applications of Solid State Chemical Sensors*, CRC Press, Boca Raton, FL, 1977, pp. 81–87.

[19] S.I. Leppävuori and P.S. Romppainen, The use of hybrid microelectronics in the construction of ion-selective electrodes, *Electrocomponent Sci. Technol., 10* (1983) 129–133.
[20] S.A. Wring, J.P. Hart and B.J. Birch, Voltammetric behavior of screen-printed carbon electrodes, chemically modified with selected mediators, and their application as sensors for the determination of reduced glutathione, *Analyst, 116* (1991) 123–129.
[21] D.H. Craston, C.P. Jones, D.E. Williams and N.E. Murr, Microband electrodes fabricated by screen printing processes: applications in electroanalysis, *Talanta, 38* (1991) 17–26.
[22] C.S. Cha, M.J. Shao and C.C. Liu, Electrochemical behavior of microfabricated thick-film electrodes, *Sensors and Actuators B, 2* (1990) 277–281.
[23] R.E. Trease and R.L. Dietz, Rheology of pastes in thick-film printing, *Solid-State Technol.*, (Jan.) (1972) 39–43.
[24] L.F. Miller, Screenability and rheology, *Solid-State Technol.*, (Oct.) (1974) 54–60.
[25] N. Hampp, C. Eppelsheim, J. Popp, M. Bisenberg and C. Bräuchle, Design and application of thick-film multisensors, *Sensors and Actuators A, 31* (1992) 144–148.
[26] T. Matsuo and H. Nakajima, Characteristics of reference electrodes using a polymer gate, *Sensors and Actuators, 5* (1984) 293–305.
[27] S. Yee, H. Jin and L. Lam, Miniature liquid junction reference electrode with micromachined silicon cavity, *Sensors and Actuators, 15* (1988) 337–345.
[28] R.L. Smith and D.C. Scott, An integrated sensor for electrochemical measurements, *IEE Trans. Biomed. Eng., BME-33* (1986) 83–90.
[29] C.P. Wong, High performance screen printable silicone as selective hybrid IC encapsulant, *IEEE Trans. Components, Hybrids, Manufact. Technol., CHMT-13* (1990) 759–765.
[30] Y. Sano, Advanced polyimide passivation technology on semiconductor wafer by screen printing method, *Epo-Tek Tech. Seminar '89, Epoxy Technology Inc., Billerica, MA, USA, June 21, 1989*, pp. 1–13.
[31] Y. Umezawa (ed.), *CRC Handbook of Ion-Selective Electrodes: Selectivity Coefficients*, CRC Press, Boca Raton, 1990.
[32] A. Sibbald, P.D. Whalley and A.K. Covington, A miniature flow-through cell with a four-function CHEMFET integrated circuit for simultaneous measurements of potassium, hydrogen, calcium and sodium ions, *Anal. Chim. Acta, 159* (1984) 47–62.
[33] I.R. Lauks, M.R. Groves and H.J. Wieck, Mass fabricated ion, gas, and enzyme multispecies sensors using IC technology, *Proc. Symp. Electrochemical Sensors Biomed. Appl., Boston, MA, USA, 1986*, pp. 116–128.
[34] N. Ho, J. Kratochvil, G. Blackburn and J. Jinata, Encapsulation of polymeric membrane-based ion-selective field-effect transistors, *Sensors and Actuators, 4* (1983) 413–421.
[35] H. van den Vlekkert, M. Decroux and N. de Rooij, Glass encapsulation of chemical solid state sensors based on anodic bonding, *Tech. Digest, 4th Int. Conf. Solid-State Sensors and Actuators (Transducers '87), Tokyo, Japan, June 2–5, 1987*, pp. 730–733.
[36] K. Potje-Kamloth, P. Jinata, J. Jinata and M. Josowicz, Electrochemical encapsulation for sensors, *Sensors and Actuators, 18* (1989) 415–425.

Biographies

Howard D. Goldberg received his B.S. degree in electrical engineering from Lehigh University in 1987. He received his M.S. degree (1989) and his Ph.D. (1993) in electrical engineering, with an emphasis on solid-state electronics, from the University of Michigan. His Ph.D. work was concerned with improving the reliability and lifetimes of solid-contact potentiometric chemical sensors as well as the development of a new mass-fabrication sequence for integrated solid-state chemical-sensor arrays with on-chip analog and digital circuitry. Howard is currently a postdoctoral associate at the Microsystems Technology Laboratories at the Massachusetts Institute of Technology. His current research interests involve the design and fabrication of novel micromechanical sensors and actuators.

Richard B. Brown received B.S. and M.S. degrees in electrical engineering from Brigham Young University in 1976. From 1976 to 1981 he worked in computer design as vice-president research and development at Holman Industries, Oakdale, CA, and then as manager of computer development at Cardinal Industries, Webb City, MO. Richard received an electrical engineering Ph.D. at the University of Utah in 1985. His Ph.D. work was in the area of solid-state chemical sensors, which included development of a custom MOS fabrication process and integration of multiple transducers with analog and digital circuitry. In September 1985, he joined the University of Michigan Department of Electrical Engineering and Computer Science faculty. He has been involved in shaping the VLSI program there and introducing a uniform set of electronic CAD tools into the curriculum. His areas of current research are high-speed digital integrated circuits and solid-state sensors.

Dong P. Liu received her B.S. degree in chemistry from the University of Science and Technology of China in 1986. In 1989, she received her M.S. in medicinal chemistry from Beijing Medical University. She is currently working toward her Ph.D. degree in electroanalytical chemistry at the University of Michigan, under the guidance of Professor Mark E. Meyerhoff.

Mark E. Meyerhoff, professor of chemistry at the University of Michigan, received his B.A. degree in chemistry from the Herbert H. Lehman College (SUNY System) in 1974 and his Ph.D. degree from the State University of New York at Buffalo in 1979. Following a brief period as a postdoctoral fellow at the University of Delaware, he joined the faculty at Michigan as an assistant professor in the Fall of 1979. His research interests are in the field of analytical chemistry, particularly the development of new ion-, gas-, and bio-selective electrochemical sensors suitable for clinical and environmental measurements. He also has active

research programs in the analytical areas of enzyme-linked competitive binding assays and ion-chromatography. He has authored or co-authored more than 100 original research articles on these subjects and is on the editorial or advisory boards of several journals devoted to the field of analytical chemistry. He is a member of the American Chemical Society, the American Association for the Advancement of Science, the American Association of Clinical Chemists, and the Alpha Chi Sigma Chemical Fraternity.